

SOIL-FOUNDATION-STRUCTURE PROBLEMS RELATED TO TRAIN-INDUCED VIBRATIONS – THE KINEMATIC INTERACTION OF TUNNEL EXCITED PILE FOUNDATIONS AND THE INERTIAL INTERACTION OF HIGH-RISE BUILDINGS

L. Auersch¹

¹ Federal Institute of Material Research and Testing
Unter den Eichen 87, Berlin 12200
e-mail: lutz.auersch-saworski@bam.de

Abstract

The soil-foundation-structure interaction is always important when building vibrations due to train passages have to be considered. The frequency range for train vibrations is up to 100 Hz. Normally, soft surface soils are crucial so that the wavelength can be much smaller than the foundation dimensions. Three topics are of interest for the prediction and the understanding of building vibrations. 1. The „kinematic interaction“ or the „added foundation effect“, which is calculated either by the combined boundary-element finite-element method or by the wavenumber domain method, results in a reduction of the free-field vibration. The stiffness of the foundation resists the wave deformation, plates and walls for horizontally propagating waves or piles for vertically incident waves. 2. The „inertial interaction“ or the „added building effect“ yields an amplification around the vertical building resonance, which may be a rigid mode on the compliant soil or a flexible mode for high-rise buildings, and a reduction at higher frequencies. This has been analysed by detailed finite element models of apartment and office buildings. 3. Base isolation is a method to further reduce building vibrations. It is important to know the soil-foundation impedance for the possible reduction, as well as the correct building impedance. A high-rise building cannot be considered as a rigid mass model. It has a frequency-dependent behaviour with longitudinal waves travelling from the foundation to the top of the building which include the effect of floor vibrations. Experiences from building projects in Vienna, Frankfurt and Berlin will give some additional results for the excitation from tunnel lines, the kinematic response of pile foundations, and the inertial response of the flexible multi-storey buildings.

Keywords: Kinematic Interaction, Inertial Interaction, Surface Foundation, Pile Foundation, High-Rise Building.

1 INTRODUCTION

The problem is outlined in Figure 1. A building is founded on pile foundations and is excited by trains in a nearby tunnel. The problem is usually divided in the “kinematic interaction” and the “inertial interaction”. The kinematic interaction, this is the reduction of the free field waves by a stiff foundation, is firstly analysed for surface foundations and secondly for pile foundations. The inertial interaction where the building-soil model is analysed for a uniform excitation, is then presented for three building examples.

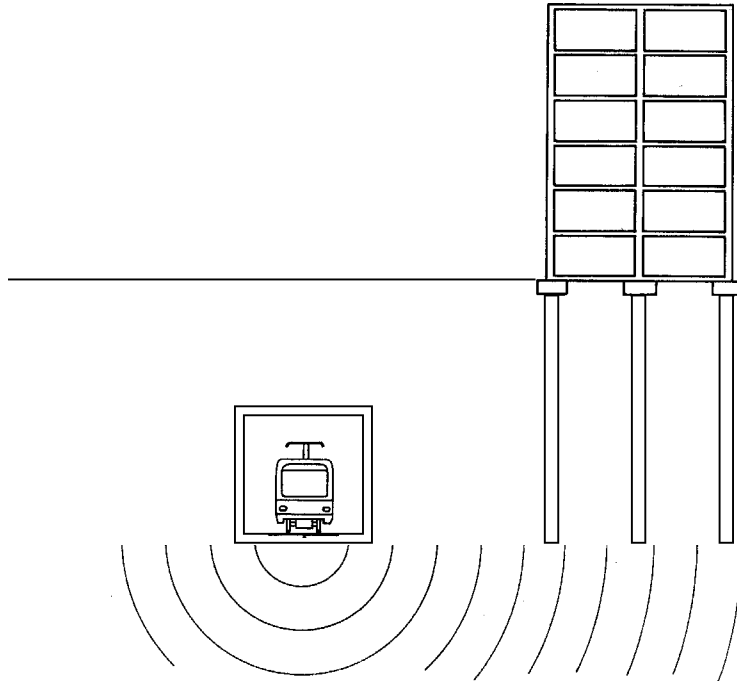


Figure 1: Train-induced building vibration, from the tunnel to the pile foundation into the multi-storey building.

2 THE COMBINATION OF THE FINITE-ELEMENT AND THE BOUNDARY-ELEMENT METHOD FOR THE SOIL-STRUCTURE INTERACTION

The behaviour (the dynamic stiffness and the kinematic interaction) of the foundation is calculated by the boundary-element method where the stiffness of a flexible foundation (beam, plate, wall) can be modelled by finite elements. In general, the whole building could also be modelled within the coupled FEBEM [1], but the large examples (tower buildings) presented here have been calculated with a commercial finite element software.

The boundary element method yields the frequency-dependent, complex dynamic stiffness matrix $\mathbf{K}_S(\omega)$ of the soil, where $\omega = 2\pi f$ is the circular frequency. The foundation (or building) structure is modelled by the finite element method. The global finite-element stiffness and mass matrices \mathbf{K}_0 and \mathbf{M} yield also a frequency-dependent dynamic stiffness matrix $\mathbf{K}_F(\omega)$ of the foundation

$$\mathbf{K}_F(\omega) = \mathbf{K}_0 - \omega^2 \mathbf{M} \quad (1)$$

The dynamic stiffness matrices of the soil and the structure are added to yield the global dynamic stiffness matrix $\mathbf{K}_{FS}(\omega)$

$$\mathbf{K}_{FS}(\omega) = \mathbf{K}_F(\omega) + \mathbf{K}_S(\omega) \quad (2)$$

of the combined foundation-soil system. The equation

$$\mathbf{K}_{FS}(\omega) \mathbf{u}(\omega) = \mathbf{p}(\omega) \quad (3)$$

of dynamic soil-structure interaction is solved to get the global displacements $\mathbf{u}(\omega)$ for any external global force excitation $\mathbf{p}(\omega)$.

In case of a free-field excitation $\mathbf{u}_0(\omega)$ of the soil, the equation

$$\mathbf{K}_{FS}(\omega) \mathbf{u}_F(\omega) = \mathbf{K}_S(\omega) \mathbf{u}_0(\omega) \quad (4)$$

has to be solved for the “kinematic interaction”. A similar equation holds for the “inertial interaction” of the building-foundation system

$$\mathbf{K}_{BF}(\omega) \mathbf{u}(\omega) = \mathbf{K}_F^*(\omega) \mathbf{u}_F(\omega) \quad (5)$$

where the dynamic stiffness $\mathbf{K}_F(\omega)$ of the foundation is approximated by a number of spring and damper elements as $\mathbf{K}_F^*(\omega)$.

3 KINEMATIC INTERACTION OR ADDED FOUNDATION EFFECT

3.1 Beams, plates, and walls under horizontal wave excitation

The surface foundations are analysed for some standard parameters, the shear modulus $G = 8 \cdot 10^7 \text{ N/m}^2$, the shear wave velocity $v_S = 200 \text{ m/s}$, and the compressional wave velocity $v_P = 400 \text{ m/s}$ of the soil, the elasticity modulus of concrete $E = 3 \cdot 10^{10} \text{ N/m}^2$, and the length of the foundation $L = 20 \text{ m}$. The width ($a = 0.2, 0.5, 20 \text{ m}$) and the height (between 0.5 and 20 m) are varied with the different types of foundation. The free-field excitation u_0 is a horizontally propagating wave with the Rayleigh wave velocity of $v_R = 186 \text{ m/s}$.

At first, beams of different heights are presented in Figure 2a. The frequency-dependent transfer functions u/u_0 (for the centre of the foundation) start with the value 1 and decreases with increasing frequency. The reduction of the free-field depends strongly on the bending stiffness of the beams. For a beam height of 0.5 m, the reduction at 30 Hz is only 0.6 whereas for a beam with $h = 1.5 \text{ m}$ (with a 30 times higher bending stiffness), the reduction reaches values smaller than 0.1 already at 25 Hz. The decrease (the slope) of this curve is also the strongest of all four curves.

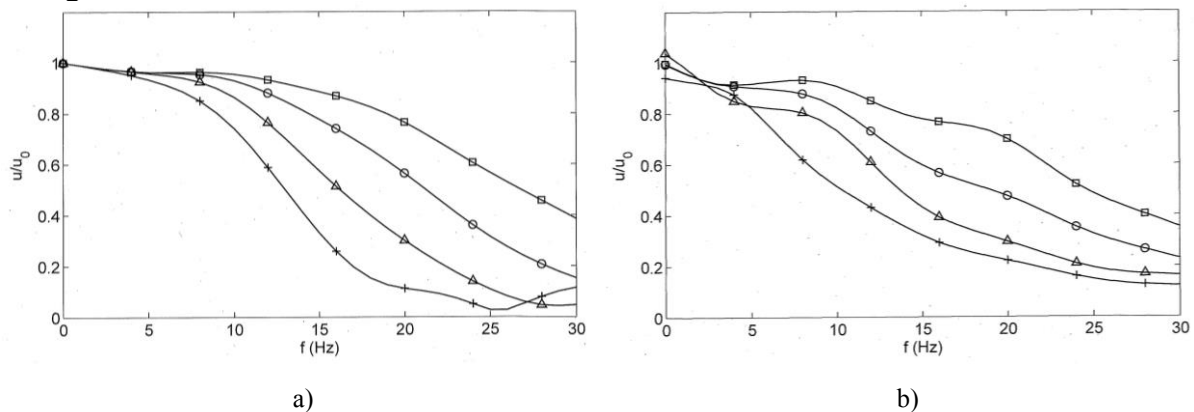


Figure 2: Transfer function u/u_0 of a) concrete beams ($a = 0.5 \text{ m}$, $L = 20 \text{ m}$), b) concrete plates ($a = 20 \text{ m}$, $L = 20 \text{ m}$), with different heights $h = \square 0.5, \circ 0.7, \triangle 1.0, + 1.5 \text{ m}$, excited by a horizontally propagating wave.

Figure 2b shows comparable results for plate foundations with the same heights. The reduction is stronger than the reduction of the beams as far as the lower frequencies up to 15 Hz are observed. For higher frequencies, the beams have steeper curves and lower values. The higher soil-plate transfer values are due to the strong radiation damping for the wide soil area under the plate which is not present for the narrow beam foundation.

Next, low walls, which may exist in basement floors, are examined with Figure 3a for different masonry walls and a concrete wall. The reduction of the horizontally propagating waves is strongest for the stiffest material, the concrete. The reduction starts at low frequen-

cies and reaches values of 0.1 already at 10 Hz. The masonry walls reach their strongest reduction at about 20 Hz.

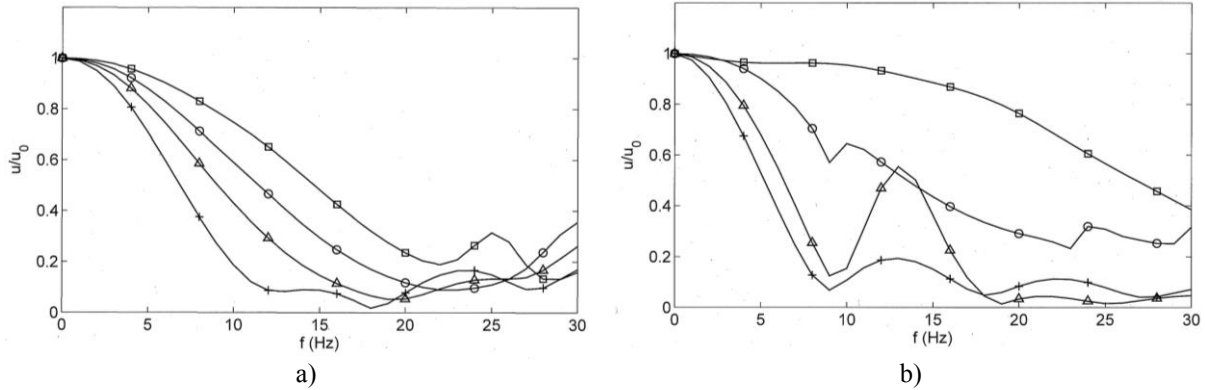


Figure 3: Transfer function u/u_0 of a) low walls ($H = 5$ m, $a = 0.2$ m, $L = 20$ m), with different $G = \square$ 1, \circ 2, \triangle 4, $+$ 13 10^9 N/m², b) high walls with $G = \circ$ 1, \triangle 13 10^9 N/m², \square low beam ($h = a = 0.5$ m, $L = 20$ m), $+$ rigid massless foundation ($L = 20$ m), excited by a horizontally propagating wave.

Finally, high walls (20 m x 20 m large) are considered in Figure 3b. The behaviour of a soft masonry wall (circle markers) is completely different from the behaviour of a concrete wall (triangle markers). The reduction is quite similar to the low masonry wall with a continuously decreasing curve. The concrete wall, however, shows a strongly frequency-dependent behaviour. Zeros occur at 19 and 26 Hz and a strong maximum at 13 Hz. For comparison, the reduction of the smallest concrete beam and of a rigid (massless) foundation are also presented in Figure 3b. It can be understood that the high concrete wall responds like a rigid, but massive foundation which has the same zeros as the massless foundation and in addition an amplification at the wall-soil resonance frequency.

3.2 Rigid surface foundations and piles under horizontal and vertical wave excitation

A finite rigid foundation subjected to the wave-field excitation of a homogeneous soil can be calculated approximately by the simple formula of the kinematic interaction

$$\frac{u}{u_0} = \int_{-L^*/2}^{L^*/2} \exp ix^* dx^* / L^*/2 = \frac{\sin L^*/2}{L^*/2} \quad (6)$$

where $L^* = L\omega/v_R$. In Figure 3b, the curve with the plus markers shows the cancelation of the waves for a 20 m long foundation, which occurs at 9, 18 and 28 Hz if 1, 2 or 3 wavelengths fit into the foundation length. The length is the most relevant parameter for the wave reduction of a rigid foundation.

A similar formula holds for a rigid pile of length H which is excited by a vertically incident P-wave. A second P-wave must be considered which is reflected at the stress-free surface of the soil. The superposition of these two waves yields a standing wave, and the average amplitude of this standing wave is

$$\frac{u}{u_0} = \int_0^{L^*} \cos z^* dz^* / H^* = \frac{\sin H^*}{H^*} \quad (7)$$

where $H^* = H\omega/v_P$. Formula (7) is similar to formula (6) but the full length H of the pile is effective instead half the length L of the beam, and the compressional wave velocity v_P is used instead of the Rayleigh wave velocity v_R . Formula (7) holds for an earthquake excitation (see also Appendix A).

If the pile is excited by a metro train (a vertical point load at finite depth), the situation is more complex (Figure 4a presents the situation for a 10 m long rigid pile and the source at 30 m depth). The point load excites P- and S-waves travelling vertically upwards, which show strong interferences for the free field (square markers). Moreover, there is an attenuation (to

half the amplitude in the present case) from entering of the incident wave to the exit of the reflected wave. Figure 4 compares the amplitudes (admittances v/F) of the free field with the pile response at the soil surface (circle markers). There is a strong reduction for frequencies above 10 Hz. The maximum ratio would be 1/3, but the minimum values are nearly 0 at 14 and 28 Hz. These minima are at higher frequencies than for an earthquake excitation where minima at 10, 20 and 30 Hz are expected from equation (7).

Contrary, if the source is close to the pile end (at a depth of 11 m in Figure 4b), an amplification of the free field occurs instead of a reduction. This is due to the strong attenuation of the free field from 1 m (where the pile is excited) to 11 m distance of the soil surface to the source.

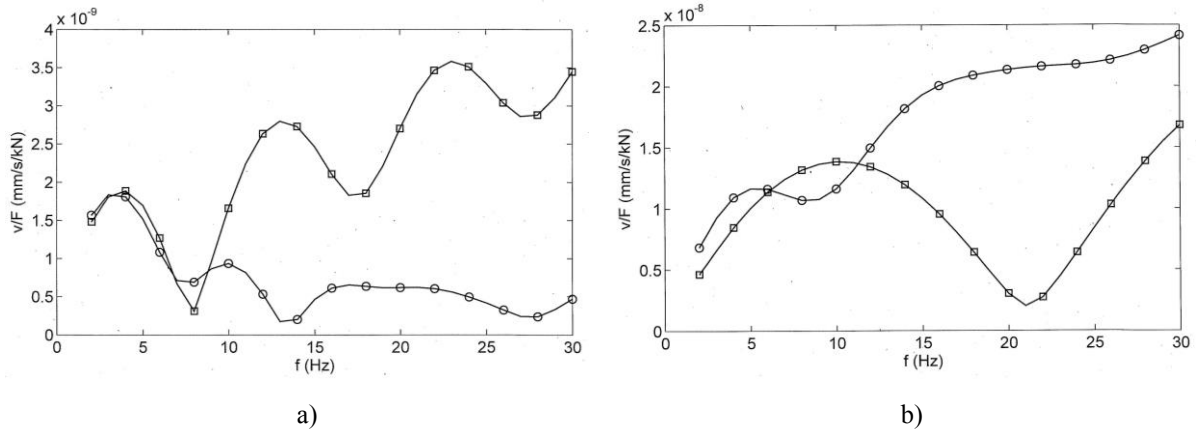


Figure 4: Admittance functions v/F of a rigid pile of length $H = 10$ m excited by the vertically propagating wave field from a point load at depth $z_0 =$ a) 30 m (far field), and b) 11 m (near field), \square free field, \circ response of the pile at the soil surface.

3.3 Pile groups under horizontal wave excitation

The following pile groups are considered [2]: A shallow foundation and a single pile for comparison, a line of 10 piles for theoretical studies, a circle of 16 piles (motivated by a wind

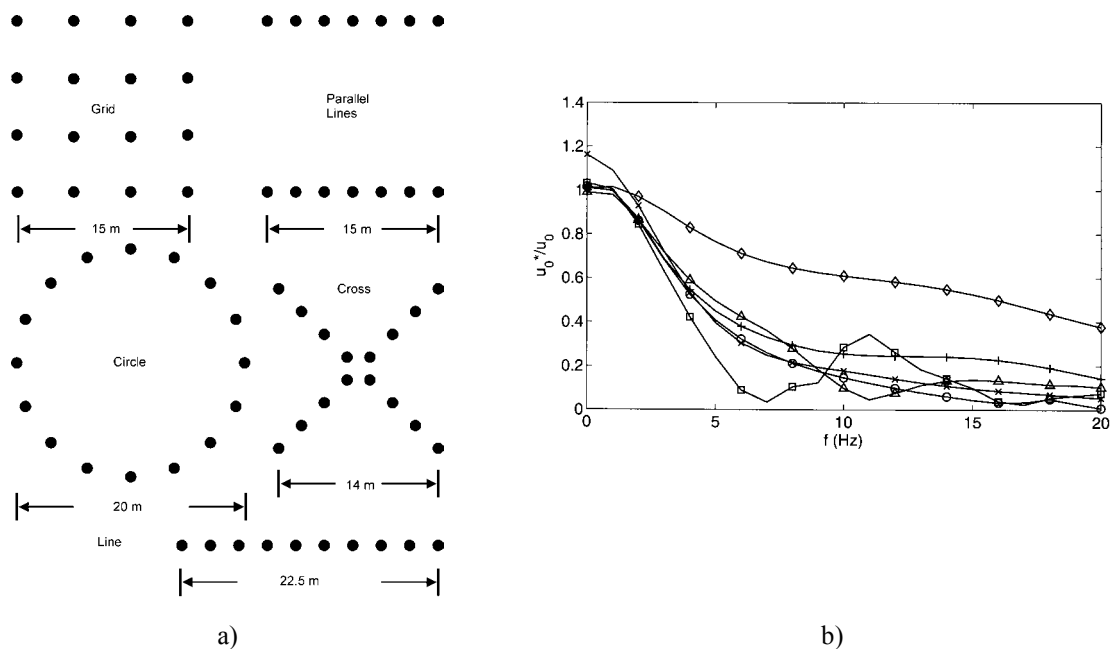


Figure 5: Rigid pile groups (a) excited by a horizontally propagating wave, b) transfer functions u_0^*/u_0 for a \square circle, \circ grid, \triangle parallels, $+$ cross, \times line, \diamond single pile, ($H = 20$ m, $2R = 1$ m).

energy plant), two parallel lines of 2 x 7 piles (as a simple case of a building above a railway or motorway tunnel), a regular grid of 16 piles (typical for residential and office buildings), and a cross of 16 piles as a not so regular building foundation. The detailed dimension can be taken from Figure 5a. The diameter $2R$ of the circular piles is 1 m and the length H is 20 m. The area which is covered by the pile groups is approximately $15 \text{ m} \times 15 \text{ m} = 225 \text{ m}^2$. The excitation is a vertical point load at 20 m horizontal distance from the centre of the pile group. The kinematic interaction is described as the amplitude ratio between the response of the massless rigid foundation and the amplitude of the free field (Fig. 5b). The response at the free surface at the centre of the pile group (that is in 20 m distance of the loading point) is used as the reference u_0 . In case of the single pile, the kinematic effect is due to the averaging of the different amplitudes at different depths which leads only to a moderate reduction of $u/u_0 \approx 0.4$ at 20 Hz. For all pile groups with rigidly connected piles, there are strong phase differences between the different foundation points. The averaging of amplitudes with different phases yields a strong reduction. Reductions down to $u/u_0 \approx 0.1$ are observed at 20 Hz, and the amplitudes clearly continue to decrease with increasing frequency.

4 INERTIAL INTERACTION OR ADDED BUILDING EFFECT

The effect of the building mass on the ground vibration has been called the “inertial interaction”. As the simplest model, a rigid building can be added to the foundation model. Real buildings and namely high-rise buildings behave quite different from a rigid mass. An example for a six-storey apartment building with concrete walls is shown in Figure 6a. Longitudinal waves are propagating from the foundation to the roof and floor resonances (at 20 Hz) modify considerably the soil-building transfer functions. At 20 Hz, the floor resonance causes a minimum of the wall, and for frequencies higher than 32 Hz the different storeys behave different, minima can be found at different frequencies (higher frequencies for higher storeys), and the amplitudes vary around a constant value. In contrary, the rigid building models, which have been calculated for different soils (Fig. 6b) and different buildings (Fig. 6c), show a uniform strong decrease of amplitudes.

The same difference between the rigid and flexible modelling can be seen for buildings on different base isolations where the realistic high-frequency reduction (Fig. 6e) is considerably over-predicted by the rigid building model (Fig. 6d). A smooth prediction model for the average building amplitudes is suggested with Figure 6f, see Section 6.

Figure 7 shows the transfer functions of a 20-storey office tower calculated by the 1-dimensional soil-column-floor model

$$\frac{u_W}{u_0} = \frac{\cos a\xi}{\cos a} \frac{1}{1 + iq \tan a} \quad (8)$$

with ξ indicating the storey, a a normalised frequency parameter (which includes the stiffness of the columns and the effective mass of the floors), and q a soil-structure interaction parameter (approximately the impedance ratio between columns and foundation), see [3]. The high-rise column-type building shows a clearer building-soil resonance at 3-4 Hz where amplitudes are increasing with the height in the building. At high frequencies, the amplitudes show a reduction which is stronger with increasing height in the building. This is due to the scattering damping of the floor slabs which has been added as a portion of the point impedance

$$\frac{F}{v} = 8\sqrt{Bm''} \quad (9)$$

of an infinite floor slab with bending stiffness B and mass per area m'' . Because of all these specialties of multi-storey buildings, detailed building models have been calculated under a uniform free-field excitation for several building projects, see the three examples in the following Section 5.

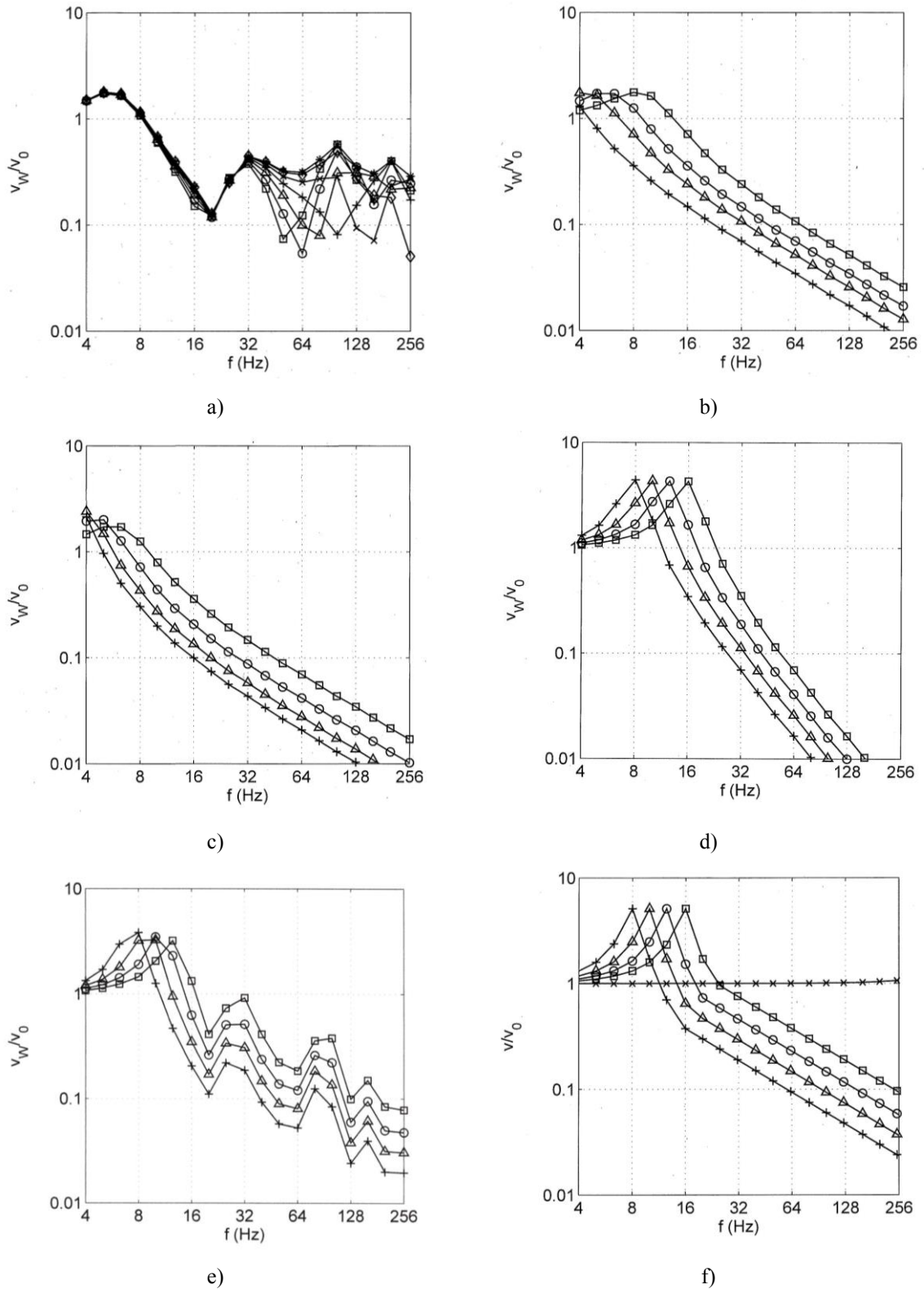


Figure 6: Transfer function v/v_0 of a six-storey apartment building a) at the 1st, 2nd, 3rd, 4th, 5th, and 6th floor, b,c) rigid buildings for soils with $v_S = 300, 200, 150, 100$ m/s (b), 6, 10, 15, + 20 storeys (c), d-f) the same building on a base isolation with $f_0 = 16, 12.5, 10, 8$ Hz, d) rigid building, e) the building with flexible walls and floors, f) a simplified model consisting of a rigid mass at low frequencies and of an infinite building at high frequencies.

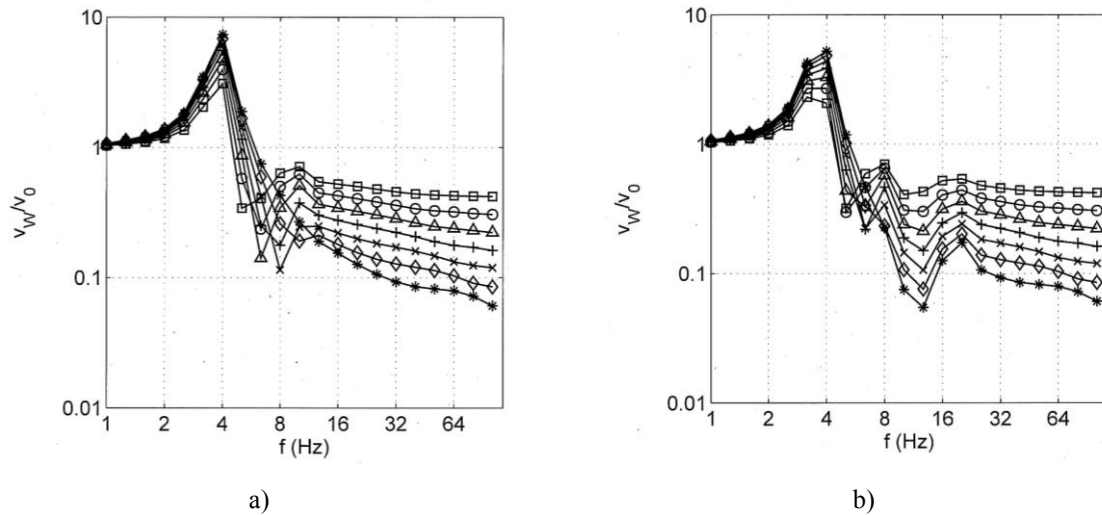


Figure 7: Transfer function v/v_0 of a 20-storey office tower at the \square 1st, \circ 4th, \triangle 7th, $+$ 10th, \times 13th, and \diamond 16th, \star 19th floor, e) model with rigid floors below $f_0 = 10$ Hz and floor dampers above, f) with floor resonance below $2f_0 = 20$ Hz and floor dampers above.

5 BUILDING EXAMPLES

5.1 Frankfort tower

A 40-storey tower in Frankfort has been analysed for the excitation by a metro tunnel in 10 m distance. The pile foundation consists of 50 piles of $H = 40$ m and $R = 1$ m which are connected by a 3 m thick concrete plate. The tower is founded on a stiff soil of $v_s = 400$ m/s. The following foundation details can be taken from the analysis of Section 3.3. The values of the kinematic effect of the pile groups (Fig. 5) can be transferred to the present case by multiplying the frequencies by 2. In addition, the compliance (stiffness) of a single pile can be taken from Appendix A (Fig. 11b) as well as the group effect of 1/6 for the stiffness and 1 for the damping (Fig. 12).

The response of the whole soil-building system (the “inertial interaction effect”) is calculated by a detailed finite-element model (Figure 8a). The building vibrations are quite different for the core, the near core areas, and the column areas. An average amplitude over several points has been built for every fifth storey and is presented for frequencies between 1 and 100 Hz as one-third octave spectra (Fig. 8b). A resonance amplification of up to $V = 6$ is observed at 2 to 3 Hz where the amplitudes are clearly increasing with the height in the building. At high frequencies, a completely different behaviour can be found, the amplitudes decrease with increasing storey with 0.5 dB per storey. This attenuation is a result of the structural damping of the walls and columns, and of the scattering damping of the floors. The attenuation is stronger if the material damping of the building material is increased to 5 % (Fig. 8c). The attenuation is also stronger if the excitation is only applied at the first row of piles (Fig. 8d). The latter results in a general reduction by the stiff foundation slab, but also to a scatter of waves through the floors which is considerably stronger than for the uniform excitation of all piles (Fig. 8b,c). Therefore, the attenuation with increasing storey starts at a lower frequency of 12 Hz and reaches a stronger value of more than 1 dB per storey (Fig. 8d).

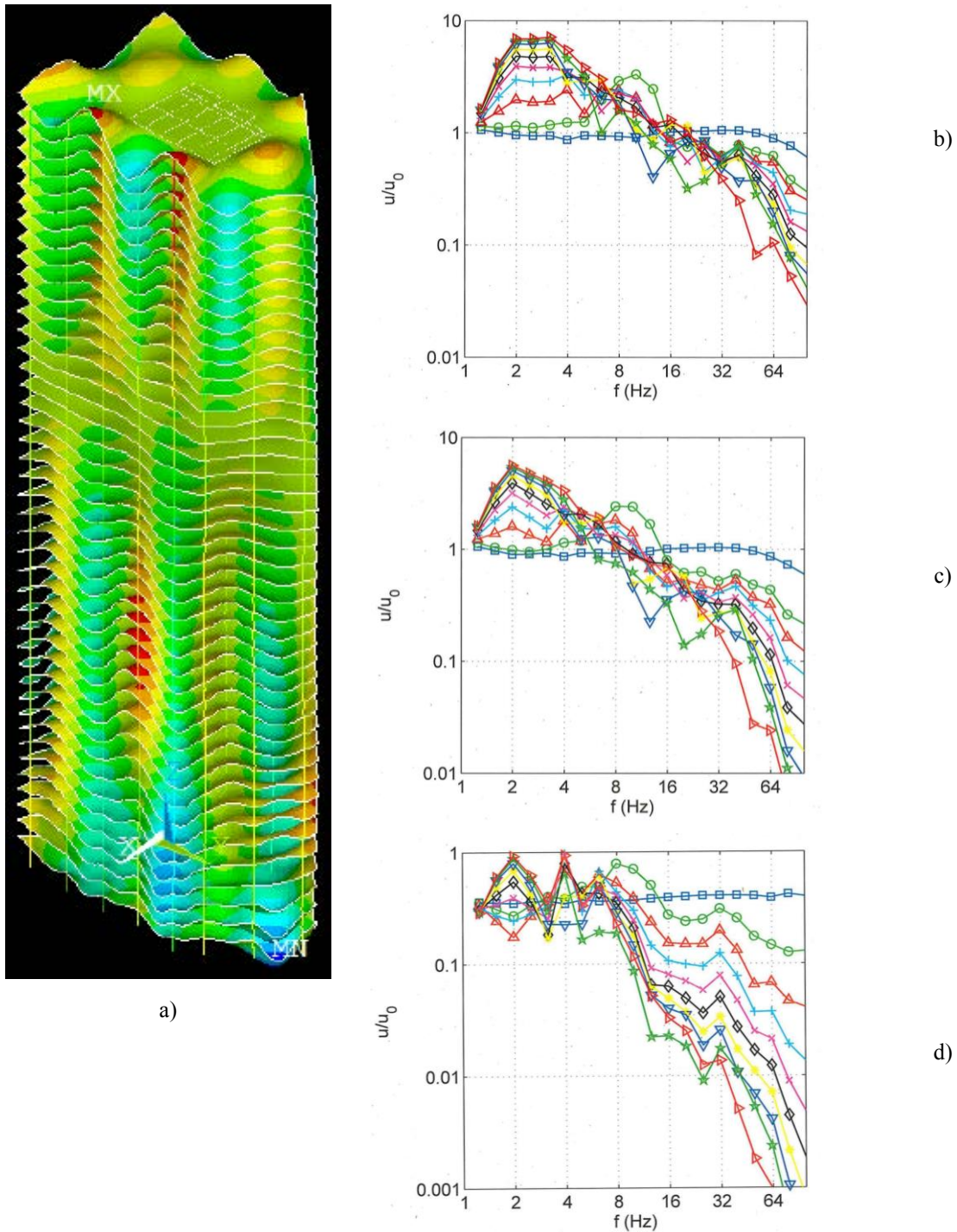


Figure 8: 40-storey Frankfort tower, a) vibration mode at 10 Hz, b) transfer functions u/u_0 of the building-soil system under uniform free-field excitation, \square base plate, \circ ground floor, \triangle 5th, $+$ 10th, \times 15th, \diamond 20th, $*$ 25th, ∇ 30th, \star 35th, \triangleright 40th storey, c) increased structural damping of 5%, d) increased scattering damping of the floors (only one row of piles excited).

The scattering damping of the floor slabs has also been included in the 1-dimensional soil-column-floor model, and the results for a 20-storey office tower clearly show the attenuation with increasing storey number (Fig. 7).

5.2 Hotel “Berlin Alexanderplatz”

The hotel consists of a 10-storey part and a 20-storey part (Fig. 9a). The metro is passing below the outer floors of the 10-storey part which is founded on piles. The vibration mode at 8 Hz (Fig. 9b) clearly shows that the central columns of both parts show a resonance amplification. The different parts of the building behave quite different although the model has been calculated for a uniform excitation. The wall has no amplification (Fig. 9c) whereas the column has a strong amplification at 10 Hz (Fig. 9d). At medium frequencies (40 – 60 Hz), the wall shows a characteristic spread of amplitudes, and the amplitudes are attenuated with increasing height at high frequencies. The different behaviour of different building parts seems to be a general characteristic of multi-storey buildings as has been found from a parameter study in [4].

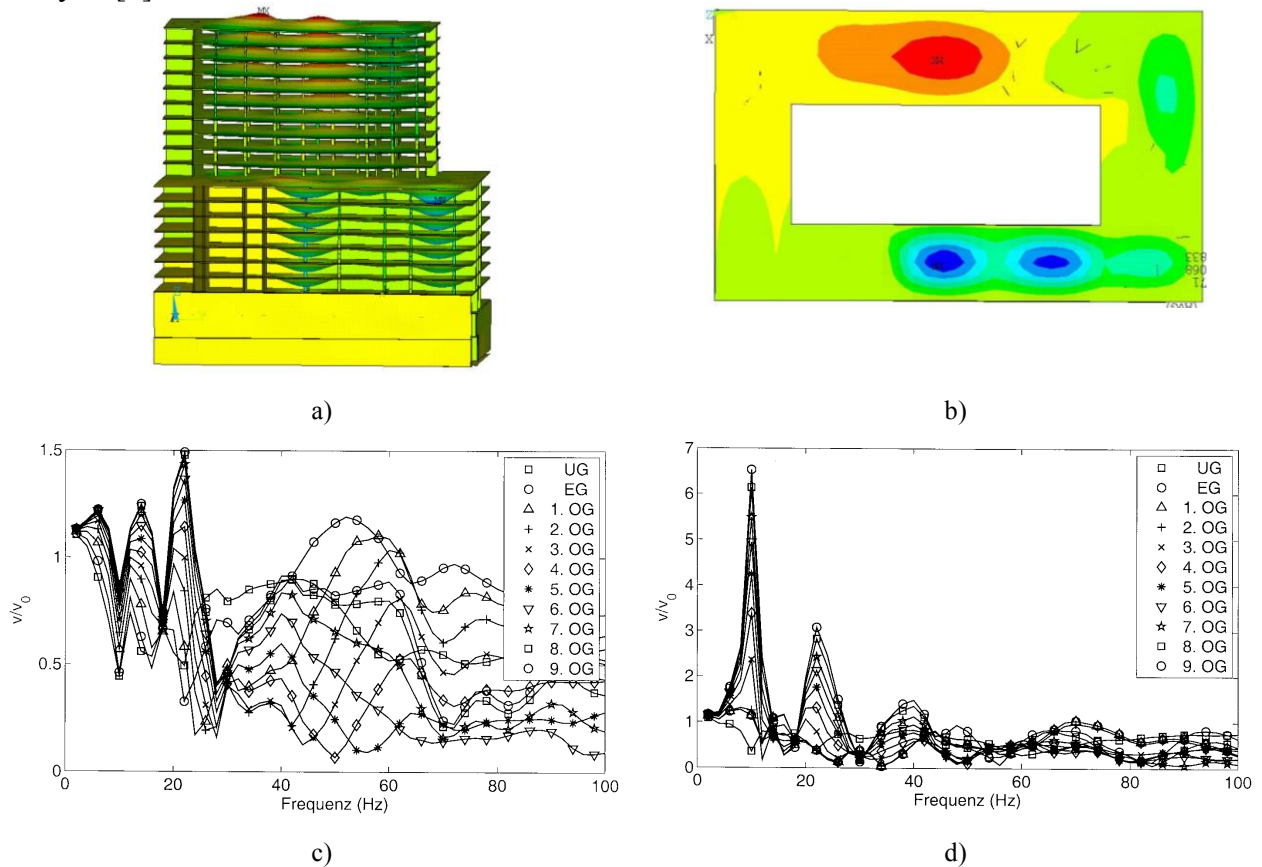


Figure 9: Hotel “Berlin Alexanderplatz” with 10- and 20-storey parts, calculated vibration mode at, a) 12 Hz, side view, b) 8 Hz, top view, c) transfer functions of a wall, d) transfer functions of a column.

5.3 City Tower Vienna

The vibrations of the 24-storey City Tower Vienna have been calculated and measured for trains running under the building (Fig. 10a,b). The transfer functions are shown in Figure 10c,d. The measurements and calculations show in good agreement the resonance amplification at about 6 Hz which is increasing with the height within the building. Moreover, the resonance amplifications of the floors between 10 and 20 Hz are also in good agreement.

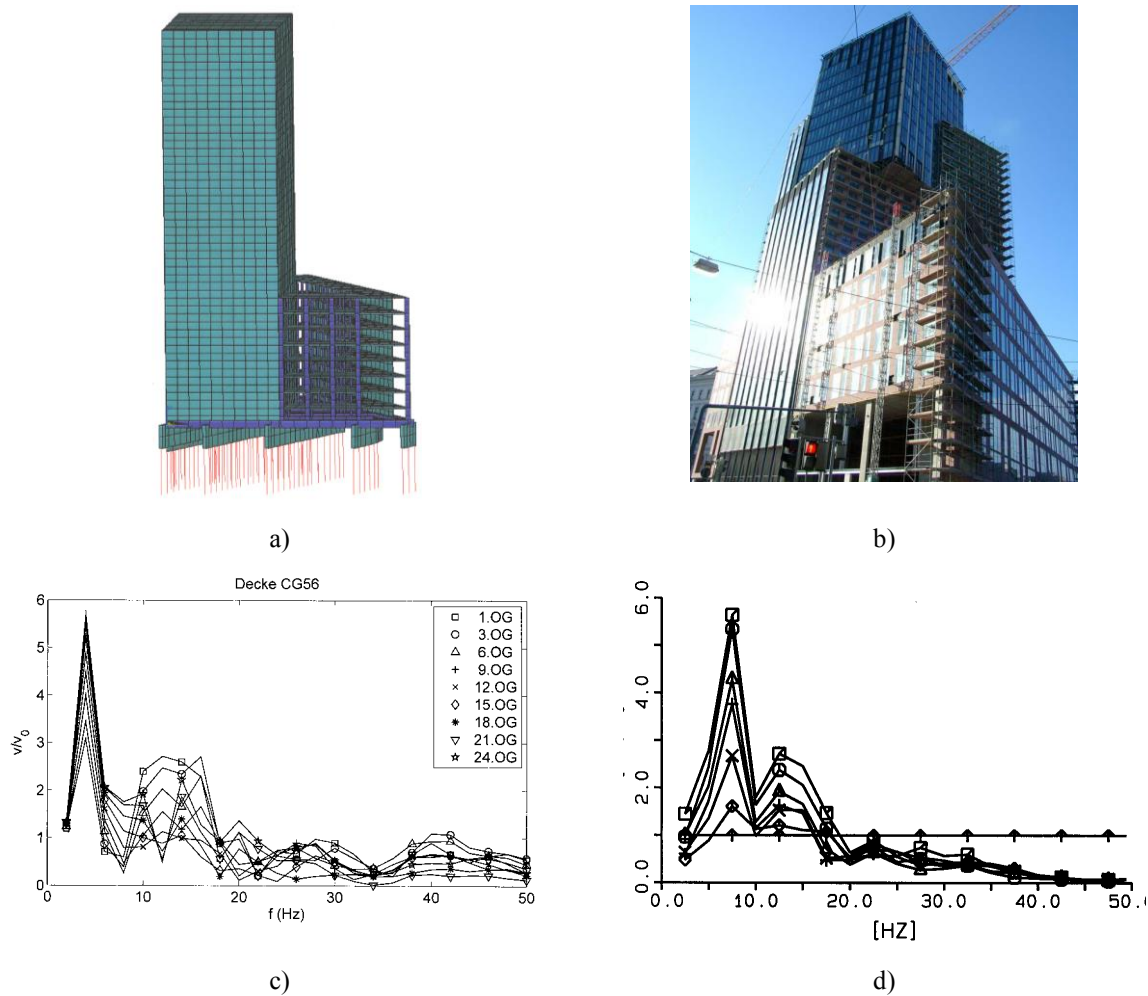


Figure 10: 24-storey City Tower Vienna (b), finite element model (a), calculated transfer functions (c), measured transfer functions (d, \square 24th, \circ 21st, \triangle 18th, $+$ 15th, \times 12th, \diamond 6th, \blacktriangle ground storey)

6 BASE ISOLATION OF A BUILDING

Base isolations are often characterised by a frequency f_0 , which is the resonance frequency of the rigid building on the isolation system. The reduction effect of a base isolation, however, should not be calculated by a rigid building model as neither the resonance frequency nor the reduction values are correct. This is demonstrated by Figures 6d and 6e where the frequency f_0 is varied between 8 and 16 Hz. These resonance frequencies can be clearly seen for the rigid building (Fig. 6d). Compared to the the strong reduction of the rigid building, the reduction of the flexible building is considerably weaker (Fig. 6e). The floor masses vibrate with the whole building at low frequencies. Then the floor resonance frequency at 20 Hz (with maximum of the floor response, not shown) is observed as a minimum of the wall response. Above the resonance frequency, the floor masses are decoupled from the building. Moreover, higher storeys are also decoupled from the lower building so that the reduction effect of the base isolation is weaker than for the full rigid mass. For a better prediction of the isolation effect, a different simple model can be used [5] which consists of a rigid building for the low frequencies and an infinitely high building for the high frequencies (Fig. 6f).

7 CONCLUSION

The kinematic reduction of the free field by stiff or rigid foundations has been presented for beams, plates low and high walls under horizontally propagating Rayleigh waves (see more results in [6]), and for piles under vertically incident compression waves. Reductions to 10 to 30 % of the free field are usually found at 30 Hz. Additional high-frequency reductions are due to the inertial interaction where a complete building-soil model has been calculated under a uniform free-field excitation. The amplitudes decrease with increasing height in the building due to the material damping and the scattering damping of the floors. At low frequencies, however, the amplitudes are amplified compared to the free field, increasing with the storey number. The prediction of the effect of a base isolation should regard these effects of a flexible building.

8 ACKNOWLEDGEMENT

M. Eidenmüller from ITA helped with the modelling and calculation of the Frankfurt tower. My colleagues W. Wuttke and W. Schmid did the hard job of installing 120 sensors in the Vienna City Tower (without a lift!). Thanks to S. Said who helped with measuring, evaluating, modelling and calculating for several building projects in Berlin and Vienna.

REFERENCES

- [1] L. Auersch, G. Schmid, A simple boundary element formulation and its application to wavefield excited soil-structure interaction. *Earthquake Engineering and Structural Dynamics*, **19**, 931–947, 1990.
- [2] L. Auersch, Wave propagation in the elastic half-space due to an interior load and its application to ground vibration problems and buildings on pile foundations. *Soil Dynamics and Earthquake Engineering*, **30**, 925–936, 2010.
- [3] L. Auersch, Building response due to ground vibration – simple prediction model based on experience with detailed models and measurements. *International Journal of Acoustics and Vibrations*, **15**, 101–112, 2010.
- [4] L. Auersch, S. Ziemens, The response of different buildings to free-field excitation – a study using detailed finite element models. M. Papadrakakis, eds. *EURODYN 2020*, Athens, Greece, November 23–26, 2020, 4560–4576.
- [5] L. Auersch, Prediction of building noise and vibration – 3D finite element and 1D wave propagation models. *Proceedings of Euronoise 2021*, LNEC, Lisbon, 2021.
- [6] L. Auersch, G. Sanitate, Effetto filtro esercitato dalle plate e pareti su onde incidente orizzontalmente. *Rivista Italiana di Geotecnica*, submitted 2023.

9 APPENDIX A: RIGID AND FLEXIBLE PILES AND PILE GROUPS UNDER VERTICAL WAVE AND FORCE EXCITATION

At first, a single pile is considered under a vertical earthquake excitation. A compressional wave is incident from infinity. The transfer function between the free field (incident and reflected wave) and the pile response is shown in Figure 11a for different pile materials. Strong variations with frequency can be found for the stiff piles, most clearly for the rigid pile (diamond marker). The flexible piles reach a different limit case, the infinitely long pile which is almost reached for the curve with square markers. This curve can be read as a function of the dimensionless frequency parameter $H^* = \omega H/v_P$, where 20 Hz relates to $H^* = 2\pi$. The stiffness ratio between pile and soil must be expressed as h/H with the elastic length h

$$h = \sqrt{\frac{EA}{G}} \quad (10)$$

of the pile according to the correct dimensional analysis. The stiffness or length ratios of Figure 11 are 0.5, 0.7, 1.0, 1.5, 2.5, and infinity for the rigid pile. The infinitely long flexible limit can be read from the curve with the square markers where $f = 20$ Hz corresponds to $h^* = \omega h/v_P = \pi$.

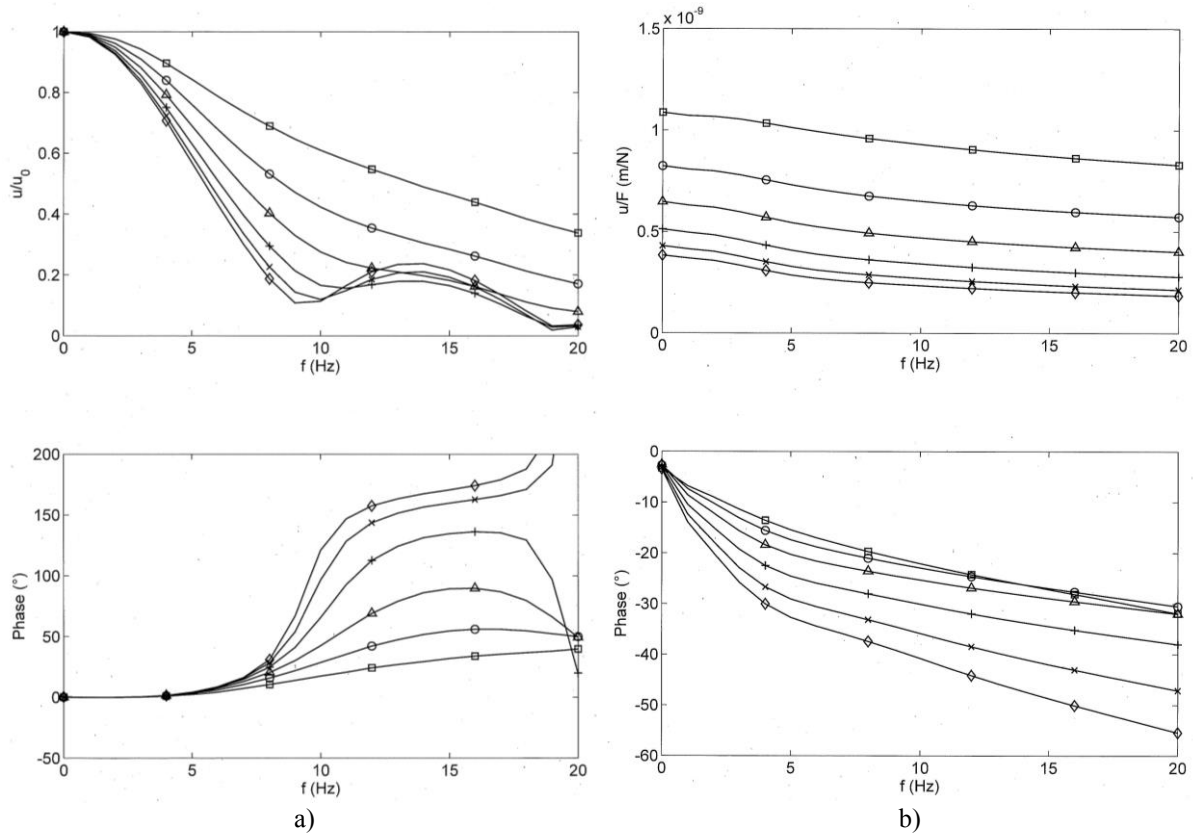


Figure 11: Transfer functions u/u_0 resp. u/F for single piles under a) earthquake and b) force excitation, pile material with $E = \square$ 0.7, \circ 1.5, \triangle 3.0 (concrete), $+$ 7, \times 21 10^{10} N/m² (steel), \diamond ∞ (rigid), ($H = 20$ m, $2R = 1$ m), amplitude (top), phase (bottom).

The same single piles are considered under a vertical force excitation in Figure 11b. The same limit cases can be observed. The non-dimensional compliances should be read from this figure as $C^* = uGH/F$ (≈ 0.6) for the rigid pile (diamond marker) and as $C^{**} = uGh/F$ (≈ 0.7) for the infinitely long flexible pile (square markers) where the static values are given in bra-

ckets. For higher values of h/H , the “rigid” limit is approached from above, for lower values the “infinitely long flexible” limit is approached also from above. The higher phase delays indicate the stronger damping of the stiff piles.

In Figure 12, groups of rigid and flexible piles are examined (see Figure 5a for the different configurations). The compliances are considerably frequency dependent, namely for the “grid” and “parallel” configurations. A general strong decrease of the amplitudes is found, and phases around 90° indicate that the damping is dominant. The results for the flexible (concrete) piles (Fig. 12b) are quite similar to the results for the rigid piles (Fig. 12a). The amplitudes are somewhat higher, and the phase (the damping) is reduced.

A group of n piles has a higher compliance than n single piles acting together. This group effect yields a factor of 5 to 7 for the different pile groups [2]. As the damping has (almost) no group effect, it becomes more dominant for the pile groups.

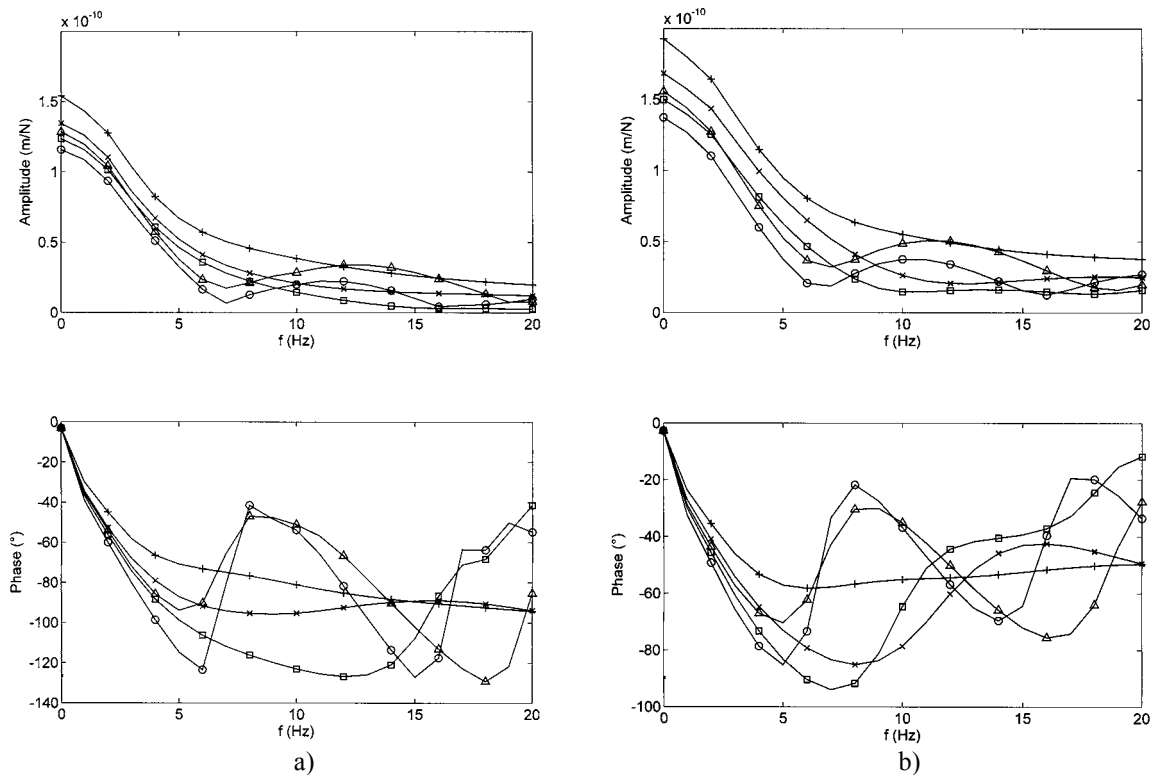


Figure 12: Groups of rigid (a) and flexible (b) pile groups excited by a vertical force, compliances u/F for a \square circle, \circ grid, \triangle parallels, $+$ cross, \times line, \diamond single pile, ($H = 20$ m, $2R = 1$ m), amplitude (top), phase (bottom).